HHS Public Access

Author manuscript

Life Sci. Author manuscript; available in PMC 2024 October 17.

Published in final edited form as:

Life Sci. 2023 May 15; 321: 121608. doi:10.1016/j.lfs.2023.121608.

TRIM21 ubiquitylates GPX4 and promotes ferroptosis to aggravate ischemia/reperfusion-induced acute kidney injury

Xiaolin Sun[a], **Ning Huang**[a], **Peng Li**[a], **Xinyi Dong**[a], **Jiahong Yang**[a], **Xuemei Zhang**[a], **Wei-Xing Zong**[b], **Shenglan Gao**[c], **Hong Xin**[a,*]

[a]Department of Pharmacology, School of Pharmacy, Fudan University, Shanghai 201203, China

[b]Department of Chemical Biology, Ernest Mario School of Pharmacy, Rutgers University, Piscataway, NJ 08854, USA

[c]Department of Cellular and Genetic Medicine, School of Basic Medical Sciences, Fudan University, Shanghai 200032, China

Abstract

Aims: This study aims to verify the molecular mechanism that Tripartite motif containing 21 (TRIM21) promotes ubiquitination degradation of glutathione peroxidase 4 (GPX4) by regulating ferroptosis, and to discuss the feasibility of TRIM21 as a new therapeutic target for acute kidney injury (AKI).

Materials and methods: Ischemia-reperfusion (I/R)-AKI model was constructed using *Trim21*$^{+/+}$ and *Trim21*$^{-/-}$ mice, and the expression of markers associated with kidney injury and ferroptosis were evaluated. HK-2 cells were treated by RSL3 and Erastin, and a hypoxia/reoxygenation (H/R) model was constructed to simulate I/R injury *in vivo*.

Key findings: *In vivo*, TRIM21 is highly expressed in I/R kidney tissues. Loss of TRIM21 alleviated I/R-AKI and improved renal function. The upregulation of GPX4, a key ferroptosis regulator, and the mild mitochondrial damage suggested that loss of TRIM21 had a negative regulation of ferroptosis. *In vitro*, TRIM21 was highly expressed in H/R models, and overexpression of TRIM21 in HK-2 cells increased ROS production, promoted intracellular iron accumulation, and boosted cellular sensitivity to RSL3 and Erastin. Mechanistically, we confirmed that GPX4 is a substrate of TRIM21 and can be degraded by TRIM21-mediated ubiquitination, suggesting that inhibiting TRIM21 attenuates ferroptosis. A JAK2 inhibitor Fedratinib downregulated TRIM21 expression and reduced damage both *in vivo* and *in vitro*, which is correlated with the upregulation of GPX4.

*Corresponding author at: Department of Pharmacology, School of Pharmacy, Fudan University, No.826 Zhangheng Road, Shanghai 201203, China. xinhong@fudan.edu.cn (H. Xin).

CRediT authorship contribution statement

Hong Xin: Conceptualization, Methodology, Funding acquisition. **Xiaolin Sun:** Data curation, Writing-Original draft preparation. **Ning Huang:** Visualization. **Peng Li:** Formal analysis. **Xinyi Dong:** Software, Validation. **Jiahong Yang:** Software. **Xuemei Zhang:** Writing-Reviewing and Editing. **Wei-Xing Zong:** Supervision. **Shenglan Gao:** Supervision, Funding acquisition. All authors read and approved the final manuscript.

Declaration of competing interest

The authors declare no conflicts of interest.

Significance: Our study showed that loss of TRIM21 could alleviate ferroptosis induced by I/R, revealed the mechanism of ubiquitination degradation of GPX4 by TRIM21 and suggested TRIM21 is a potential target for the treatment of AKI.

Keywords

TRIM21; GPX4; Ferroptosis; AKI; Ubiquitination degradation

1. Introduction

Acute kidney injury (AKI) is a clinical syndrome of rapid decline in renal function characterized by azotemia, electrolyte and acid-base disturbances, multiple complications, and failure of other organs [1]. Patients require long-term dialysis treatment and face concomitant complications, including chronic kidney disease (CKD) and end-stage renal disease (ESRD) [2]. No effective specific therapy for AKI has been established so far. The clinical treatment of AKI is focused mainly on dealing with its related complications. For patients with renal failure, renal replacement therapy is still the first choice for clinical treatment [3]. Therefore, it is of critical clinical significance to discover the pathogenesis and possible targets, and to explore emerging therapeutic methods for AKI treatment.

Several types of cell death including apoptosis, necrosis, autophagy, and pyroptosis have been considered pathophysiologically involved in AKI [4–6]. Ferroptosis is defined as an iron-dependent form of regulated cell death (RCD), which has been shown to be involved in AKI and ischemia/reperfusion (I/R) injury [2,7]. The mechanism of ferroptosis involves mainly the massive cell accumulation of Fe^{2+} and glutathione peroxidase 4 (GPX4) abnormality. The excessive accumulation of Fe^{2+} in cells catalyzes the Fenton reaction of unsaturated fatty acids, especially that of the unsaturated phospholipids located on the cell membrane. The abundant accumulation of lipid peroxides cannot be timely metabolized, resulting in intracellular oxidative stress and eventual cell death [8]. Ferroptosis is one of the main causes of renal tubular cell death in I/R-AKI [9]. Treatment with the ferroptosis inhibitor ferrostatin-1 (Fer-1) can effectively alleviate renal injury [10]. These results suggest that ferroptosis plays a significant role in renal injury, and targeting ferroptosis is a potential therapeutic strategy for AKI.

Tripartite motif containing 21 (TRIM21) is an E3 ubiquitin ligase which is considered to be related to antiviral responses and autoimmune diseases [11]. In addition, the role of TRIM21 in cancer progression has been observed in a number of studies [12]. Furthermore, several key molecules in inflammation-related tumorigenesis and cancer therapy have been identified as ubiquitinated substrates of TRIM21 [13]. However, it is unclear whether TRIM21 can regulate AKI. Herein, we used *Trim21*$^{-/-}$ mice and the JAK2 inhibitor Fedratinib to assess the role of TRIM21 in AKI. We discovered that TRIM21 knockout alleviates kidney injury by inhibiting ferroptosis. The potential mechanism is through the TRIM21 regulation of GPX4 ubiquitination degradation. Our findings expand the existing knowledge of the regulatory role of TRIM21 and provide a new strategy for the treatment of I/R-AKI.

2. Materials and methods

2.1. Chemical reagents

RSL3 (HY-100218A), Erastin(HY-15763), MG132 (HY-13259), Cycloheximide (CHX) (HY-12320), and Fedratinib (HY-10409) were purchased from MedChem Express (Monmouth Junction, NJ, USA). Polybrene (E1299) and puromycin (CL13900) were purchased from Selleck Chemicals (Houston, TX, USA).

2.2. Animal experiments

Trim21 KO mice with a C57BL/6J background (used in part 3.1) were kindly provided as a gift from Dr. Keiko Ozato. Only male mice were used in this study. Male C57BL/6J mice (aged 8–10 weeks; weighing 20–25 g) (used in part 3.6) were purchased from LINGCHANG BIOTECH (China). Mice were housed in a 12 h day-night cycle room and allowed chow and water freely. The animal procedures were approved by the Animal Care and Use Committee of Fudan University (Shanghai, China).

Mice were fasted for 12 h and anesthetized (1 % pentobarbital sodium, i.p.) before surgery. Bilateral renal pedicles were clamped for 30 min, then remove the arterial clamps. The sham groups were treated in the same way, except for the clamping of the renal pedicle. Blood samples were collected 24 h after reperfusion, mice were killed, and kidney were collected for follow-up experiments. Fedratinib (5 mg/kg body weight) was injected (i.p.) into mice 24 h once in advance before surgery.

2.3. Renal functional parameters

Renal function is reflected by serum creatinine (CRE) and blood urea nitrogen (BUN) levels, which was measured using the Creatinine Assay Kit (Jiancheng, Nanjing, China) and BUN Assay Kit (Jiancheng, Nanjing, China), respectively, according to the manufacturer's protocols.

2.4. Mitochondrial morphology observation by electron microscopy

The renal cortices were cut into small pieces (1 mm^3) and quickly placed in electron microscopy fixative at 4 °C. Then the samples were dehydrated and embedded and then stained with uranyl acetate and lead citrate. Renal tubular epithelial cells were observed by transmission electron microscopy and images were collected.

2.5. Histology and immunohistochemistry analyses

Renal tissues were fixed and processed for hematoxylin and eosin (H&E) and immunohistochemistry staining for TRIM21. In brief, renal tissues were fixed in 4 % paraformaldehyde overnight, embedded in paraffin, sliced, and stained with H&E according to standard procedures. The renal tubular damages were quantitated in 10 randomly selected fields. Evidence of brush border loss, dilatation, formation, necrosis of renal tubules, and neutrophil infiltration were scored from 0 to 5 (0: normal; 1: <11 %; 2: 11 %–25 %; 3: 26 %–45 %; 4: 46 %–75 %; 5: >75 %). Evaluations were carried out by three researchers who did not know how each group was treated. Statistical analysis was carried out after averaging the scores of the three researchers. Immunohistochemistry staining was

performed as described previously [14], and an antibody against TRIM21 (1:100; 12108–1-AP; Proteintech) was used.

2.6. Malondialdehyde (MDA) and GSH/GSSG Assay

The MDA levels and the GSH/GSSG levels in kidney tissues were measured using a Lipid Peroxidation MDA Assay Kit (Beyotime Institute of Biotechnology, Shanghai, China) and a GSH and GSSG Assay Kit (Beyotime Institute of Biotechnology, Shanghai, China), respectively, according to the manufacturer's instructions.

2.7. Cell culture and in vitro treatment

HK-2 cell line was purchased from American Type Culture Collection (Manassas, VT, USA). HK-2 cells were cultured in Dulbecco's modified Eagle's medium (DMEM)/F12 supplemented with 10 % fetal bovine serum (FBS) and 1 % penicillin-streptomycin in an incubator with 5 % CO_2 at 37 °C. For induction of the cell model of H/R, HK-2 cells were incubated in a hypoxia incubator with 1 % O_2, 94 % N_2, and 5 % CO_2 for 24 h at 37 °C, then the cells were replaced into normoxic conditions for 6 h. Cells maintained in normoxic conditions were cultured in 5 % CO_2 and 95 % air at 37 °C as controls.

2.8. Evaluation of cell viability

Cell viability was measured using the Enhanced Cell Counting Kit-8 (CCK-8) (Beyotime Institute of Biotechnology, Shanghai, China). HK-2 cells were seeded in 96-well plates to different treatment for 24 h, the culture media was added with 10 μL/well CCK-8 solution and incubated at 37 °C for 2 h. The absorbance values at 450 nm were detected by a microplate reader (Thermo Fisher Scientific, Waltham, MA, USA).

2.9. Western blot

Electrophoresis was performed using 8 %–12 % SDS polyacrylamide gels. Proteins were transferred to polyvinylidene difluoride (PVDF) membranes and blocked for 2 h using 5 % skimmed milk and Tris-buffered saline and Tween 20 (TBST) buffer. Then membranes were incubated overnight at 4 °C with the following primary antibodies: GPX4 (1:4000; ab125066; Abcam), ferritin heavy chain 1 (FTH1) (1:1000; 4393; Cell Signaling Technology), TRIM21 (1:2000; ab207728; Abcam), acyl-CoA synthetase long-chain family member 4 (ACSL4) (1:2000; A6826; Abclonal), solute carrier family 7 member 11 (SLC7A11) (1:1000; 12691; Cell Signaling Technology), GAPDH (1:5000; 10494-1-AP; Proteintech), Ubiquitin (1:1500; 10201-2-AP; Proteintech), JAK2 (1:1000; 3230; Cell Signaling Technology), Phospho-JAK2 (Y1007 + Y1008) (1:5000; ab32101; Abcam), STAT3 (1:2000; WL03207; Wanlei), and Phospho-STAT3 (Tyr705) (1:2000; 3772; Cell Signaling Technology). After a reaction with the primary antibodies, the PVDF membranes were incubated with horseradish peroxidase-conjugated secondary antibodies for 2 h at room temperature. Then the immune complexes were detected using ECL solution, and the values of each band was determined using Image Lab (Bio-Rad Laboratories, Hercules, CA, USA).

2.10. Real time quantitative PCR

Total RNA was extracted using Trizol reagent (Invitrogen, USA). RNA was reverse transcribed to cDNA using the PrimeScript™ RT Master Mix (TaKaRa, China). Gene expression was determined with an SYBR-Green (TaKaRa, China) PCR assay in a CFXTM Real-Time Thermal cycler (Bio-Rad, Hercules, CA). The primers used are listed in Table 1. Data were analyzed by the $2^{-\Delta\Delta Ct}$ method, normalized to GAPDH or β-actin, and compared with the control.

2.11. Measurement of intracellular reactive oxygen species (ROS) levels

The intracellular ROS levels were detected using the Reactive Oxygen Species Assay Kit (Beyotime Institute of Biotechnology, Shanghai, China). After treatment, cells were incubated with DCFH-DA fluorescent probe (2 μM) in the dark at 37 °C for 20 min, and the ROS level was measured with a CytoFlex S flow cytometer (Beckman Coulter, Brea, CA, USA).

2.12. Measurement of intracellular iron levels

The intracellular iron levels were detected using calcein acetoxymethyl ester (calcein-AM) (Yeasen, Shanghai, China) [15]. The binding of iron ions causes fluorescence quenching. After treatment, cells were incubated with calcein-AM (0.5 μM) in the dark at 37 °C for 15 min, and the fluorescence intensity was measured with a CytoFLex S flow cytometer (Beckman Coulter, Brea, CA, USA).

2.13. Transient transfection, lentiviral infection

Transient transfections for plasmids were performed according to the protocol of Lipofectamine 3000 (Thermo Fisher Scientific, CA, USA).

Procedure for building stable overexpression cell lines and knockdown cell lines: HEK293T cells were seed in six-well plates. After overnight recovery, for stable overexpression cell lines and knockdown cell lines, cells were transfected with lentivirus plasmid and packaging system. Preparation of Lipo3000 diluent (tube A): After absorbing 250 μL opti-MEM, adding Lipo3000 (7.5 μL), mixing and standing at room temperature. The mixture for preparing the plasmid (tube B): After absorbing 250 μL opti-MEM, adding destination DNA (2.5 μg), packing plasmid (2.25 μg), P3000 6 μL, mixing and standing at room temperature. Tube A and tube B were gently blown and mixed, incubated for 10–15 min and then added to the cells by drops. Replace the media according to the instructions and collect the virus-containing medium, the virus-containing medium was mixed with complete DMEM/F12 medium at a ratio of 1:1, The HK-2 cells were cultured with viral medium containing 0.1 % polybrene, and selected by puromycin (2 mg/mL) for 3 days. The information on plasmids used is listed in Table 2.

2.14. Immunofluorescence

HK-2 cells were plated on the confocal dish at a density of 5×10^5 cells/well. After 24 h, Vehicle or Fedratinib was added and placed in an anoxic incubator for 24 h, then placed in a normal incubator for 6 h to construct H/R injury. Cells were fixed with 4 %

formaldehyde for 15 min at room temperature (RT). The cells were then permeabilized with 0.3 % Triton X-100 for 10 min, and non-specific binding sites were blocked by blocking solution (Beyotime Institute of Biotechnology, Shanghai, China) for 1 h. The cells were then incubated with primary antibodies, TRIM21 (1:50; 12108-1-AP; Proteintech) and GPX4 (1:400; 67763-1-lg; Proteintech) overnight at 4 °C. After washed with PBS (3 × 5 min), the secondary antibodies conjugated to Alexa Fluor 555 (Beyotime Institute of Biotechnology, Shanghai, China) and Alexa Fluor 488 (Beyotime Institute of Biotechnology, Shanghai, China) were applied at RT for 1.5 h. The cells were then stained with DAPI (Beyotime Institute of Biotechnology, Shanghai, China) at RT for 5 min, followed by mounting and examination with a laser scanning confocal microscope (Olympus, Japan).

2.15. Co-immunoprecipitation (Co-IP)

Cells were lysed with IP Lysis Buffer (Beyotime Institute of Biotechnology, Shanghai, China). Protein A/G agarose beads (Bimake, Houston, Texas, USA) were incubated with the lysate supernatant in a rolling incubator for 2 h. Then the beads were discarded and the appropriate antibodies, IgG (3 μg; 6990; Cell Signaling Technology), TRIM21 (3 μg; 12108-1-AP; Proteintech), and GPX4 (3 μg; A11243; Abclonal), were added. Incubated overnight at 4 °C in the rolling incubator. Added fresh beads and incubated in the rolling incubator at 4 °C for 2 h. Discard beads and add 1× loading buffer, then boiling for 5 min. The bound proteins were detected by western blot analysis.

2.16. Statistical analyses

Quantitative experimental data are expressed as mean ± SD. Statistical analyses were undertaken using Prism 8 (GraphPad, San Diego, CA, USA). For analysis between two groups, a student *t*-test was applied. One-way ANOVA with Tukey's post-hoc test was employed for comparisons between more than two groups. A value of $p < 0.05$ was considered to indicate a statistically significant difference.

3. Results

3.1. Loss of TRIM21 alleviates I/R-induced renal injury in vivo

We explored the expression profile of Trim21 in I/R-AKI. A data set containing RNA-seq data by comparing I/R and sham surgery samples from the GEO database (GSE98622) was used in this study [16]. Elevated *Trim21* mRNA level was observed in I/R tissues compared with sham tissues both at 24 h and 12 months (Fig. 1A). We constructed an I/R-AKI model in $Trim21^{+/+}$ and $Trim21^{-/-}$ mice and verified this finding using western blot. The protein level of TRIM21 was increased in the WT-I/R group compared with the WT-Sham group (Fig. 1B). We further examined renal function. H&E staining revealed $Trim21^{-/-}$ alleviated the renal injury. In the WT-I/R group, the renal tubular epithelial cells were severely shed, the tubular basement membrane was significantly exposed, casts were formed, and renal interstitial edema were observed. The KO-I/R group had less damage (Fig. 1C, D). I/R caused a significant decline in renal function, which showed a significant increase in the ratio of renal weight to body weight, serum levels of CRE and BUN. Compared to the WT-I/R group, the ratio of renal weight to body weight, serum levels of CRE and BUN were lower in the KO-I/R group. (Fig. 1E, F). Similarly, mRNA expression of molecular markers

of tubular injury, KIM-1 and NGAL was suppressed in Trim21$^{-/-}$ mice (Fig. 1G). Taken together, these results suggested that Trim21$^{-/-}$ protected the kidneys from I/R damage.

3.2. Loss of TRIM21 ameliorates ferroptosis in AKI caused by I/R

I/R-AKI involves multiple injury mechanisms. Herein, we focused on exploring whether *Trim21*$^{-/-}$ could reduce kidney damage by inhibiting ferroptosis. We measured the expression of several ferroptosis biomarkers in mouse I/R models and observed a decrease in GPX4 expression, but an increase in FTH1 and ACSL4 expression. *Trim21*$^{-/-}$ significantly restored the expression of GPX4 and reversed the overexpression of FTH1 and ACSL4 (Fig. 2A, B). The experimental results of previous studies showed that I/R did not affect mouse GPX4 mRNA levels, indicating the absence of an effect on transcriptional regulation of GPX4 [17]. When ferroptosis occurs, mitochondrial structural changes were observed. The electron microscopy of the WT-I/R group showed that mitochondria shrink, mitochondrial membrane thickens and cristae decrease or disappear during ferroptosis (Fig. 2C). *Trim21*$^{-/-}$ showed mild mitochondrial damage, consistent with H&E staining in Fig. 1C. After I/R, the GSH level in the kidneys of mice was significantly decreased, but *Trim21*$^{-/-}$ significantly inhibited the reduction of the GSH level. I/R led to the deposition of MDA in the kidney, and *Trim21*$^{-/-}$ inhibited the increase of MDA levels induced by I/R (Fig. 2D). These data suggested that *Trim21*$^{-/-}$ regulated ferroptosis-related proteins, alleviated mitochondrial damage, and reduced oxidative stress. Hence, ferroptosis inhibition may be one of the mechanisms by which *Trim21*$^{-/-}$ alleviates I/R-AKI.

3.3. TRIM21 mediates the sensitivity to ferroptosis in HK-2 cells

To further clarify the role of TRIM21 in ferroptosis regulation, TRIM21^{WT} and TRIM21^{OE} HK-2 cells were treated with the ferroptosis activators RSL3 and Erastin, which inhibit the functions of GPX4 and SLC7A11, respectively, in the antioxidant system [18]. Our results showed that TRIM21 overexpression promoted RSL3- and Erastin-induced decline in cell viability; additionally, RSL3-induced cells had higher sensitivity to TRIM21 overexpression (Fig. 3A, B). Therefore, we speculate that the regulatory effect of TRIM21 on ferroptosis may be related to GPX4. Ferroptosis is accompanied by lipid peroxidation, so we investigated the role of TRIM21 in the regulation of peroxidative stress. The changes in ROS levels, detected by DCFH-DA fluorescence indicated that TRIM21 overexpression weakened the antioxidant capacity of cells (Fig. 3C, D). Similarly, we implemented flow cytometry to the detect fluorescent intensity, which confirmed our results (Fig. 3E, F). Ferroptosis is also accompanied by the changeable intracellular iron levels. Intracellular iron levels were measured using a calcein-AM fluorescence probe, upon which binding to iron ions resulted in fluorescence quenching. In the process of RSL3- and Erastin-induced ferroptosis, cells lost iron homeostasis, formed unstable iron pool, and the fluorescence intensity was weakened. The excessive accumulation of iron in TRIM21^{OE} cells can be further aggravated (Fig. 3G, H). Therefore, TRIM21 can promote ferroptosis and aggravate lipid peroxidation and the excessive accumulation of iron which are consistent with the *in vivo* results showing that *Trim21*$^{-/-}$ mice had milder kidney injury.

3.4. TRIM21 negatively regulates GPX4 at the protein level

Based on our findings that TRIM21 is involved in ferroptosis, we further explored its underlying molecular mechanism of action. GPX4 is a central regulator of ferroptosis, and TRIM21 knockout was observed to counteract the I/R-induced downregulation of the GPX4 protein levels in Fig. 2A. Therefore, we explored more comprehensive the relationship between TRIM21 and GPX4. Myc-TRIM21 transfection in HK-2 cells significantly reduced the GPX4 protein level (Fig. 4A). To determine whether TRIM21 affected GPX4 transcription, we measured the GPX4 mRNA levels in Myc-TRIM21-transfected HK-2 cells. We found that the TRIM21 mRNA level was significantly increased, but the mRNA level of GPX4 did not change significantly. Therefore, the overexpression of TRIM21 could not regulate the transcription of GPX4 (Fig. 4B). We constructed $TRIM21^{OE}$ and $TRIM21^{KD}$ HK-2 cell lines, and found the same protein expression trend as that in the Myc-TRIM21-transfected cells. Both RSL3 and Erastin inhibited the GPX4 protein in $TRIM21^{WT}$ cells, and this effect was aggravated in the $TRIM21^{OE}$ cells but rescued in the $TRIM21^{KD}$ cells (Fig. 4C–F). These results indicate that TRIM21 downregulates GPX4 at the post-transcriptional level, which further affects ferroptosis.

3.5. GPX4 is degraded by TRIM21-mediated ubiquitination

We next explored the molecular mechanism by which TRIM21 regulates GPX4. We measured the half-life of GPX4 through a CHX-chase experiment in HK-2 cells stimulated by the ferroptosis inducer RSL3, and we found that the half-life of GPX4 was shortened in the $TRIM21^{OE}$ cells (Fig. 5A). This finding suggests that TRIM21 facilitates GPX4 protein degradation. To verify whether TRIM21 is the E3 ubiquitin ligase of GPX4, we transfected different doses of Myc-TRIM21 plasmids in HK-2 cells and established a gradual decrease in the GPX4 protein level in a TRIM21 dose-dependent manner (Fig. 5B). To further confirm the aforementioned conclusion, we transfected a TRIM21 ligase-dead (LD) plasmid into HK-2 cells and found that it did not reduce the GPX4 protein level. The transfection with the TRIM21-LD plasmid increased TRIM21 expression, but no activity of its E3 ubiquitin ligase was detected, indicating that TRIM21 downregulated GPX4 through its E3 ubiquitin ligase activity, and GPX4 is the substrate of TRIM21. Eukaryotic intracellular proteins are degraded mainly through lysosomal and proteasomal pathways [19]. Notably, the proteasome inhibitor MG132 effectively restored the endogenous GPX4 levels in $TRIM21^{OE}$ HK-2 cells (Fig. 5C). As anticipated, our co-IP assay revealed a binding effect between TRIM21 and GPX4 in HK-2 cells (Fig. 5D). In addition, the ubiquitin-proteasome system was previously shown to be involved in the degradation of GPX4 during ferroptosis [20,21]. Following this logic, we found that transfecting HK-2 cells with $TRI\text{-}M21^{OE}$ markedly increased the ubiquitination of GPX4 (Fig. 5E). On the basis of these findings, we then validated the localization TRIM21 and GPX4 in HK-2 cells. Immunofluorescence staining revealed the co-localization of TRIM21 and GPX4 proteins. The spatial positions of TRIM21 (green) and GPX4 (red) were determined by visualization through DAPI (blue) dyeing (Fig. 5F). These results suggest that TRIM21 acts as an E3 ubiquitin ligase that binds to GPX4 and promotes GPX4 ubiquitination and subsequent clearance.

3.6. Fedratinib alleviates ferroptosis by inhibiting TRIM21 in vivo

We used GEO database (GSE98622) to compare the expression profiles of JAK2 and STAT3 in I/R and sham surgery samples, and found JAK2 and STAT3 were significantly higher in I/R tissues than in sham tissues 24 h after I/R (Fig. 6A). In previous studies, the JAK2/STAT3 pathway was shown to be involved in the regulation of renal function in AKI, and blocking the JAK2/STAT3 pathway inhibited the proliferation of renal tubular epithelial cells and reduced the extent of renal injury [22–25]. Nevertheless, whether inhibition of JAK2/STAT3 pathway can alleviate AKI by regulating ferroptosis has not been reported. Based on the previous experimental results that regulating TRIM21 affects ferroptosis, we tried to select a JAK2 inhibitor that can regulate TRIM21 and investigate whether it has the effect of alleviating ferroptosis. We found that the JAK2 inhibitor Fedratinib was able to significantly reduce TRIM21 protein levels in I/R tissues. And our immunohistochemistry results showed elevated TRIM21 expression levels in I/R tissues, which is consistent with the western blot result displayed in Fig. 6B. Fedratinib significantly inhibited TRIM21 expression and counteracted the I/R-induced decrease in the GPX4 and SLC7A11 expression levels (Fig. 6B–C). H&E staining results revealed mild renal pathological damage in Fedratinib group; the CRE and BUN serum levels, and the mRNA levels of the renal injury markers NGAL and KIM-1 also indicated that Fedratinib significantly alleviated I/R-AKI and improved kidney function (Fig. 6C–E). In addition, Fedratinib significantly reversed I/R-induced decreased GSH levels and increased MDA levels in kidney tissues. In general, these findings suggest that TRIM21 expression is elevated in AKI, but Fedratinib attenuates ferroptosis by inhibiting TRIM21 expression, which then alleviates AKI.

3.7. Fedratinib alleviates ferroptosis by inhibiting TRIM21 in vitro

Based on the aforementioned results, we explored the suppressive effect of JAK2 inhibitor Fedratinib on ferroptosis in RSL3-treated HK-2 cells. Fedratinib and RSL3 co-treatment for 24 h significantly reversed the decrease in the cell viability caused by RSL3 (Fig. 7A). Additionally, we developed an *in vitro* H/R model of HK-2 cells to simulate I/R injury *in vivo*. Western blot and immunofluorescence results showed a significantly increased TRIM21 expression level, whereas that of GPX4 was significantly decreased; Fedratinib reversed both expression levels (Fig. 7B, C). Therefore, our results further validated that Fedratinib alleviates ferroptosis by inhibiting the expression of TRIM21, indicating that TRIM21 plays a crucial role in AKI and ferroptosis.

4. Discussion

In our present work, we report our findings that $Trim21^{-/-}$ protected the kidneys from I/R-AKI. Besides, we found that TRIM21 was upregulated under I/R conditions and contributed to reperfusion-induced ferroptosis injury. *In vivo*, Fedratinib ameliorated renal tubular cell injury and protected renal function by inhibiting ferroptosis through TRIM21 expression downregulation. *In vitro*, the overexpression of TRIM21 exacerbated HK-2 cell death and promoted an increased release of ROS, stimulated by ferroptosis inducers. Mechanically, TRIM21 promoted ubiquitinated degradation of GPX4, thus exacerbating ferroptosis by exerting E3 ubiquitin ligase activity (Fig. 7D). Altogether, these results suggest that TRIM21

promotes I/R-AKI development and progression through ferroptosis regulation, which may serve as a therapeutic target for AKI.

As a new form of RCD, ferroptosis has been closely correlated with human diseases, especially those characterized by kidney tubular death, including that caused by I/R, folic acid nephrotoxicity, cisplatin nephrotoxicity, and rhabdomyolysis-induced AKI [26–28]. The protective effects of deferoxamine (DFO) on the renal function in AKI model directly confirmed that ferroptosis is involved in the development of AKI [29]. However, the specific mechanism of ferroptosis in renal tubular epithelial cells caused by AKI has not been fully elucidated. Apart from blood purification, few other methods are available for the prevention and treatment of AKI. Thus, the discovery and development of new treatments are critically important and urgently needed for prognosis improvement. It is expected that ferroptosis inhibition will be established as a new effective method for the treatment of AKI.

GPX4 is the central regulator of ferroptosis [30,31]. Therefore, in recent years, the search for regulatory mechanisms of the GPX4 protein level and its activity has attracted considerable research attention focused on the discovery of potential therapeutic approaches for ferroptosis-related diseases. The accumulation of ROS is an important sign of iron toxicity triggered by the Fenton reaction that leads to lipid peroxidation [32]. GPX4 can inhibit iron toxicity by reducing lipid peroxide production. Hence, the inhibition or degradation of GPX4 can directly trigger ferritin precipitation [19]. Post-translational modifications are also a form of regulation that maintains the stability of the GPX4 protein. GPX4 protein levels can be directly regulated by autophagy [33]. During Erastin-induced ferroptosis *in vitro*, GPX4 was shown to be degraded by heat shock protein 90 (HSP90)-mediated autophagy [34]. In recent years, emerged evidence has also shown that ubiquitination modification is involved in ferroptosis [35,36]. Currently, TRIM46 was identified as an E3 ubiquitin ligase of GPX4 in high glucose-induced ferroptosis in human retinal capillary endothelial cells [20]. Tang *et al* found that a member of the Nedd4 family—neural precursor cell-expressed developmentally down-regulated 4-like (NEDD4L) promoted GPX4 ubiquitination and degradation in granulosa cells [37]. In another study, LUBAC was found to catalyze GPX4 to form a linear ubiquitin chain, which is related to the existing ubiquitin chains of GPX4, such as K48 and K63 ubiquitin chains [38]. In an investigation of deubiquitination modification, OTUB1 was identified as the deubiquitination enzyme of GPX4 in a study of CST1-promoted metastasis in gastric cancer [39]. Apart from the findings of these studies, E3 ubiquitin ligases and deubiquitination enzymes of GPX4 are still largely unknown. Therefore, it is of considerable importance to find targets that regulate the ubiquitination degradation of GPX4. In the present study, we found that TRIM21 promoted GPX4 ubiquitination degradation and was involved in the ferroptosis process. Therefore, it is reasonable to expect that a similar therapeutic effect could be achieved by specifically inhibiting the enzymatic activity of TRIM21 in triggering GPX4 ubiquitination.

TRIM21 is a member of the TRIM family and has a unique RING structure that allows its functioning as an E3 ubiquitin ligase. It is widely involved in the regulation of cell cycle, differentiation, apoptosis, metabolism, and immunity [40,41]. To date, the role of TRIM21 in I/R injury is yet to be defined. In this work, high TRIM21 levels were observed in our I/R model *in vivo* and H/R model *in vitro*. TRIM21 acted as a regulator of oxidative

damage in previous studies. The knockout of TRIM21 was found to protect the heart from pressure overload-induced heart failure and the liver from arsenic-induced liver damage [42]. TRIM21-deficient cells and the liver are protected from diethylnitrosamine (DEN)-induced oxidative damage [43]. These studies indicate an antioxidant effect caused by TRIM21 depletion. A recent study showed that the E3 ubiquitin ligase TRIM21 regulated ferroptosis through the antioxidant pathway, thereby alleviating doxorubicin-induced cardiotoxicity [44]. Considering that oxidative stress and ferroptosis are key risk factors for a variety of pathological processes, we explored whether TRIM21 affected the ferroptosis-induced oxidative stress in HK-2 cells. Our results suggest that the overexpression of TRIM21 promotes RSL3- and Erastin-induced ROS production. Thus, our findings support that TRIM21 is an important regulator of oxidative stress. However, the mechanisms leading to the elevated expression levels of TRIM21 in I/R is still not clear. Nevertheless, we will explore it in depth in our future research.

There are few studies on upstream regulation of TRIM21. Considering that the JAK2 pathway is activated during I/R-AKI, we tried to screen out JAK2 inhibitors that can regulate TRIM21 and investigate whether it has the effect of alleviating ferroptosis. We found that the JAK2 inhibitor Fedratinib were able to significantly reduce TRIM21 protein levels. As a corollary, we hypothesize that JAK2 inhibitors can regulate TRIM21 through transcription, thereby affecting the subsequent translation process. According to the experimental results, STAT3 may be the transcription factor of TRIM21, which will be our focus part next.

ACSL4, an enzyme that converts fatty acid to fatty acyl-CoA esters, regulates lipid biosynthesis [45]. FTH1 is responsible for the storage of intracellular iron [46]. *In vivo* experiments, the increased expression levels of ACSL4 and FTH1 induced by I/R were also inhibited in *Trim21*$^{-/-}$ mice to some extent. Based on the changes in the mitochondrial structure and the generation of ROS, we clearly defined the regulatory role of TRIM21 in oxidative stress, and thus we only focused on GPX4 in the stage of its mechanism exploration.

Apoptosis, a common form of RCD, was also found to be involved in I/R-AKI [47]. Interestingly, ferroptosis usually occurs in the early stage of reperfusion [17], but apoptosis occurs at a later phase and increases with the prolongation of ischemia and reperfusion times [48]. TRIM21 was reported to be closely related to apoptosis [49]. Both animal models of I/R-AKI and human AKI kidney biopsies showed apoptotic changes in renal tubular epithelial cells [50]. Taken together, we cannot exclude an involvement of TRIM21 in AKI apoptosis. In our model, I/R-induced ferroptosis produced ROS and destroyed the cellular structure. We speculate these changes may partially create a precondition for apoptosis.

There are still some limitations in our study that need to be addressed. First, although TRIM21 plays a role in a variety of physiological activities, no its specific inhibitor was found in the current study. We established that JAK2 inhibitor Fedratinib downregulated TRIM21 expression and exerted a mitigating effect on ferroptosis and AKI. The mechanisms through which JAK2 inhibitors suppress TRIM21 expression will be the focus of our future studies.

5. Conclusion

In conclusion, our results indicate that TRIM21 is involved in the pathogenesis of ferroptosis and AKI by participating in the ubiquitination degradation of GPX4, suggesting that through high throughput screening targeting TRIM21, discovering small molecular compounds that can regulate TRIM21, thus new options are available not only for the relief of organ damage, but also for the treatment of oncology.

Acknowledgements

We thank Dr. Keiko Ozato (NIH) for the *Trim21* KO mouse strain [51].

Funding

This work was supported by Natural Science Foundation of Shanghai (No. 20ZR140710) and National Natural Science Foundation of China (No. 82100293).

Data availability

The data that support the findings of this study are openly available in GEO database (GSE98622).

Abbreviations:

TRIM21	tripartite motif containing 21
GPX4	glutathione peroxidase 4
AKI	acute kidney injury
I/R	ischemia/reperfusion
H/R	hypoxia/reoxygenation
CKD	chronic kidney disease
ESRD	end-stage renal disease
RCD	regulated cell death
ROS	reactive oxygen species
FTH1	ferritin heavy chain 1
ACSL4	acyl-CoA synthetase long-chain family member 4
SLC7A11	solute carrier family 7 member 11
CRE	creatinine
BUN	blood urea nitrogen
MDA	malondialdehyde
DAPI	4′,6-diamidino-2-phenylindole

DCFH-DA	2′,7′-dchlorodihydrofluorescein diacetate
PVDF	polyvinylidene difluoride
TBST	Tris-buffered saline and Tween 20
calcein-AM	calcein acetoxymethyl ester

References

[1]. K. JA, Norbert L, Diagnosis, evaluation, and management of acute kidney injury: a KDIGO summary (Part 1), Crit. Care 17 (2013).

[2]. Levey AS, James MT, Acute kidney injury, Ann. Intern. Med 167 (2017), 10.7326/aitc201711070. Itc66-itc80.

[3]. Gumbert SD, Kork F, Jackson ML, Vanga N, Ghebremichael SJ, Wang CY, Eltzschig HK, Perioperative acute kidney injury, Anesthesiology 132 (2020) 180–204, 10.1097/aln.0000000000002968. [PubMed: 31687986]

[4]. Linkermann A, Chen G, Dong G, Kunzendorf U, Krautwald S, Dong Z, Regulated cell death in AKI, J. Am. Soc. Nephrol 25 (2014) 2689–2701, 10.1681/asn.2014030262. [PubMed: 24925726]

[5]. Tang C, Livingston MJ, Liu Z, Dong Z, Autophagy in kidney homeostasis and disease, Nat. Rev. Nephrol 16 (2020) 489–508, 10.1038/s41581-020-0309-2. [PubMed: 32704047]

[6]. Liu H, Wang L, Weng X, Chen H, Du Y, Diao C, Chen Z, Liu X, Inhibition of Brd4 alleviates renal ischemia/reperfusion injury-induced apoptosis and endoplasmic reticulum stress by blocking FoxO4-mediated oxidative stress, Redox Biol. 24 (2019), 101195, 10.1016/j.redox.2019.101195. [PubMed: 31004990]

[7]. Dixon SJ, Stockwell BR, The role of iron and reactive oxygen species in cell death, Nat. Chem. Biol 10 (2014) 9–17, 10.1038/nchembio.1416. [PubMed: 24346035]

[8]. Ursini F, Maiorino M, Lipid peroxidation and ferroptosis: the role of GSH and GPx4, Free Radic. Biol. Med 152 (2020) 175–185, 10.1016/j.freeradbiomed.2020.02.027. [PubMed: 32165281]

[9]. Zhao Z, Wu J, Xu H, Zhou C, Han B, Zhu H, Hu Z, Ma Z, Ming Z, Yao Y, Zeng R, Xu G, XJB-5-131 inhibited ferroptosis in tubular epithelial cells after ischemia-reperfusion injury, Cell Death Dis. 11 (2020) 629, 10.1038/s41419-020-02871-6. [PubMed: 32796819]

[10]. Friedmann Angeli JP, Schneider M, Proneth B, Tyurina YY, Tyurin VA, Hammond VJ, Herbach N, Aichler M, Walch A, Eggenhofer E, Basavarajappa D, Rådmark O, Kobayashi S, Seibt T, Beck H, Neff F, Esposito I, Wanke R, Förster H, Yefremova O, Heinrichmeyer M, Bornkamm GW, Geissler EK, Thomas SB, Stockwell BR, O'Donnell VB, Kagan VE, Schick JA, Conrad M, Inactivation of the ferroptosis regulator Gpx4 triggers acute renal failure in mice, Nat. Cell Biol 16 (2014) 1180–1191, 10.1038/ncb3064. [PubMed: 25402683]

[11]. Foss S, Bottermann M, Jonsson A, Sandlie I, James LC, Andersen JT, TRIM21-from intracellular immunity to therapy, Front. Immunol 10 (2019) 2049, 10.3389/fimmu.2019.02049. [PubMed: 31555278]

[12]. Hatakeyama S, TRIM proteins and cancer, Nat. Rev. Cancer 11 (2011) 792–804, 10.1038/nrc3139. [PubMed: 21979307]

[13]. Chen X, Cao M, Wang P, Chu S, Li M, Hou P, Zheng J, Li Z, Bai J, The emerging roles of TRIM21 in coordinating cancer metabolism, immunity and cancer treatment, Front. Immunol 13 (2022), 968755, 10.3389/fimmu.2022.968755. [PubMed: 36159815]

[14]. Ren D, Luo J, Li Y, Zhang J, Yang J, Liu J, Zhang X, Cheng N, Xin H, Saikosaponin B2 attenuates kidney fibrosis via inhibiting the hedgehog pathway, Phytomedicine 67 (2020), 153163, 10.1016/j.phymed.2019.153163. [PubMed: 31901891]

[15]. Prus E, Fibach E, Flow cytometry measurement of the labile iron pool in human hematopoietic cells, Cytometry A 73 (2008) 22–27, 10.1002/cyto.a.20491. [PubMed: 18044720]

[16]. Liu J, Kumar S, Dolzhenko E, Alvarado GF, Guo J, Lu C, Chen Y, Li M, Dessing MC, Parvez RK, Cippà PE, Krautzberger AM, Saribekyan G, Smith AD, McMahon AP, Molecular

characterization of the transition from acute to chronic kidney injury following ischemia/reperfusion, JCI Insight 2 (2017), 10.1172/jci.insight.94716.

[17]. Chen C, Wang D, Yu Y, Zhao T, Min N, Wu Y, Kang L, Zhao Y, Du L, Zhang M, Gong J, Zhang Z, Zhang Y, Mi X, Yue S, Tan X, Legumain promotes tubular ferroptosis by facilitating chaperone-mediated autophagy of GPX4 in AKI, Cell Death Dis. 12 (2021) 65, 10.1038/s41419-020-03362-4. [PubMed: 33431801]

[18]. Tang D, Chen X, Kang R, Kroemer G, Ferroptosis: molecular mechanisms and health implications, Cell Res. 31 (2021) 107–125, 10.1038/s41422-020-00441-1. [PubMed: 33268902]

[19]. Chen X, Yu C, Kang R, Kroemer G, Tang D, Cellular degradation systems in ferroptosis, Cell Death Differ. 28 (2021) 1135–1148, 10.1038/s41418-020-00728-1. [PubMed: 33462411]

[20]. Zhang J, Qiu Q, Wang H, Chen C, Luo D, TRIM46 contributes to high glucose-induced ferroptosis and cell growth inhibition in human retinal capillary endothelial cells by facilitating GPX4 ubiquitination, Exp. Cell Res 407 (2021), 112800, 10.1016/j.yexcr.2021.112800. [PubMed: 34487731]

[21]. Zhang W, Jiang B, Liu Y, Xu L, Wan M, Bufotalin induces ferroptosis in non-small cell lung cancer cells by facilitating the ubiquitination and degradation of GPX4, Free Radic. Biol. Med 180 (2022) 75–84, 10.1016/j.freeradbiomed.2022.01.009. [PubMed: 35038550]

[22]. Lv J, Wang X, Liu SY, Liang PF, Feng M, Zhang LL, Xu AP, Protective effect of fenofibrate in renal ischemia reperfusion injury: involved in suppressing kinase 2 (JAK2)/transcription 3 (STAT3)/p53 signaling activation, Pathol. Biol. (Paris) 63 (2015) 236–242, 10.1016/j.patbio.2015.07.010. [PubMed: 26343046]

[23]. Zhou Y, Xu W, Zhu H, CXCL8((3–72)) K11R/G31P protects against sepsis-induced acute kidney injury via NF-κB and JAK2/STAT3 pathway, Biol. Res 52 (2019) 29, 10.1186/s40659-019-0236-5. [PubMed: 31084615]

[24]. Zhu H, Wang X, Wang X, Liu B, Yuan Y, Zuo X, Curcumin attenuates inflammation and cell apoptosis through regulating NF-κB and JAK2/STAT3 signaling pathway against acute kidney injury, Cell Cycle 19 (2020) 1941–1951, 10.1080/15384101.2020.1784599. [PubMed: 32615888]

[25]. Huang F, Wang X, Xiao G, Xiao J, Loganin exerts a protective effect on ischemia-reperfusion-induced acute kidney injury by regulating JAK2/STAT3 and Nrf2/HO-1 signaling pathways, Drug Dev. Res 83 (2022) 150–157, 10.1002/ddr.21853. [PubMed: 34189758]

[26]. Vanden Berghe T, Linkermann A, Jouan-Lanhouet S, Walczak H, Vandenabeele P, Regulated necrosis: the expanding network of non-apoptotic cell death pathways, Nat. Rev. Mol. Cell Biol 15 (2014) 135–147, 10.1038/nrm3737. [PubMed: 24452471]

[27]. Fähling M, Mathia S, Paliege A, Koesters R, Mrowka R, Peters H, Persson PB, Neumayer HH, Bachmann S, Rosenberger C, Tubular von hippel-Lindau knockout protects against rhabdomyolysis-induced AKI, J Am Soc Nephrol 24 (2013) 1806–1819, 10.1681/asn.2013030281. [PubMed: 23970125]

[28]. Skouta R, Dixon SJ, Wang J, Dunn DE, Orman M, Shimada K, Rosenberg PA, Lo DC, Weinberg JM, Linkermann A, Stockwell BR, Ferrostatins inhibit oxidative lipid damage and cell death in diverse disease models, J. Am. Chem. Soc 136 (2014) 4551–4556, 10.1021/ja411006a. [PubMed: 24592866]

[29]. Shah SV, Rajapurkar MM, Baliga R, The role of catalytic iron in acute kidney injury, Clin. J. Am. Soc. Nephrol 6 (2011) 2329–2331, 10.2215/cjn.08340811. [PubMed: 21979910]

[30]. Dixon SJ, Lemberg KM, Lamprecht MR, Skouta R, Zaitsev EM, Gleason CE, Patel DN, Bauer AJ, Cantley AM, Yang WS, Morrison B III, Stockwell BR, Ferroptosis: an iron-dependent form of nonapoptotic cell death, Cell 149 (2012) 1060–1072, 10.1016/j.cell.2012.03.042. [PubMed: 22632970]

[31]. Cui C, Yang F, Li Q, Post-translational modification of GPX4 is a promising target for treating ferroptosis-related diseases, Front. Mol. Biosci 9 (2022), 901565, 10.3389/fmolb.2022.901565. [PubMed: 35647032]

[32]. Kuang F, Liu J, Tang D, Kang R, Oxidative damage and antioxidant defense in ferroptosis, Front. Cell Dev. Biol 8 (2020), 586578, 10.3389/fcell.2020.586578. [PubMed: 33043019]

[33]. Lee JJ, Ishihara K, Notomi S, Efstathiou NE, Ueta T, Maidana D, Chen X, Iesato Y, Caligiana A, Vavvas DG, Lysosome-associated membrane protein-2 deficiency increases the risk of reactive

oxygen species-induced ferroptosis in retinal pigment epithelial cells, Biochem. Biophys. Res. Commun 521 (2020) 414–419, 10.1016/j.bbrc.2019.10.138. [PubMed: 31672277]

[34]. Wu Z, Geng Y, Lu X, Shi Y, Wu G, Zhang M, Shan B, Pan H, Yuan J, Chaperone-mediated autophagy is involved in the execution of ferroptosis, Proc. Natl. Acad. Sci. U. S. A 116 (2019) 2996–3005, 10.1073/pnas.1819728116. [PubMed: 30718432]

[35]. Rape M, Ubiquitylation at the crossroads of development and disease, Nat. Rev. Mol. Cell Biol 19 (2018) 59–70, 10.1038/nrm.2017.83. [PubMed: 28928488]

[36]. Harrigan JA, Jacq X, Martin NM, Jackson SP, Deubiquitylating enzymes and drug discovery: emerging opportunities, Nat. Rev. Drug Discov 17 (2018) 57–78, 10.1038/nrd.2017.152. [PubMed: 28959952]

[37]. Tang H, Jiang X, Hua Y, Li H, Zhu C, Hao X, Yi M, Li L, NEDD4L facilitates granulosa cell ferroptosis by promoting GPX4 ubiquitination and degradation, Endocr. Connect (2023), 10.1530/ec-22-0459.

[38]. Dong K, Wei R, Jin T, Zhang M, Shen J, Xiang H, Shan B, Yuan J, Li Y, HOIP modulates the stability of GPx4 by linear ubiquitination, Proc. Natl. Acad. Sci. U. S. A 119 (2022), e2214227119, 10.1073/pnas.2214227119. [PubMed: 36279464]

[39]. Li D, Wang Y, Dong C, Chen T, Dong A, Ren J, Li W, Shu G, Yang J, Shen W, Qin L, Hu L, Zhou J, CST1 inhibits ferroptosis and promotes gastric cancer metastasis by regulating GPX4 protein stability via OTUB1, Oncogene (2022), 10.1038/s41388-022-02537-x.

[40]. Tomar D, Singh R, TRIM family proteins: emerging class of RING E3 ligases as regulator of NF-κB pathway, Biol. Cell 107 (2015) 22–40, 10.1111/boc.201400046. [PubMed: 25319221]

[41]. Esposito D, Koliopoulos MG, Rittinger K, Structural determinants of TRIM protein function, Biochem. Soc. Trans 45 (2017) 183–191, 10.1042/bst20160325. [PubMed: 28202672]

[42]. Pan JA, Sun Y, Jiang YP, Bott AJ, Jaber N, Dou Z, Yang B, Chen JS, Catanzaro JM, Du C, Ding WX, Diaz-Meco MT, Moscat J, Ozato K, Lin RZ, Zong WX, TRIM21 ubiquitylates SQSTM1/p62 and suppresses protein sequestration to regulate redox homeostasis, Mol. Cell 61 (2016) 720–733, 10.1016/j.molcel.2016.02.007. [PubMed: 26942676]

[43]. Wang F, Zhang Y, Shen J, Yang B, Dai W, Yan J, Maimouni S, Daguplo HQ, Coppola S, Gao Y, Wang Y, Du Z, Peng K, Liu H, Zhang Q, Tang F, Wang P, Gao S, Wang Y, Ding WX, Guo G, Wang F, Zong WX, The ubiquitin E3 ligase TRIM21 promotes hepatocarcinogenesis by suppressing the p62-Keap1-Nrf2 antioxidant pathway, cell Mol, Gastroenterol. Hepatol 11 (2021) 1369–1385, 10.1016/j.jcmgh.2021.01.007. [PubMed: 33482392]

[44]. Hou K, Shen J, Yan J, Zhai C, Zhang J, Pan JA, Zhang Y, Jiang Y, Wang Y, Lin RZ, Cong H, Gao S, Zong WX, Loss of TRIM21 alleviates cardiotoxicity by suppressing ferroptosis induced by the chemotherapeutic agent doxorubicin 69 (2021), 103456, 10.1016/j.ebiom.2021.103456.

[45]. Yuan H, Li X, Zhang X, Kang R, Tang D, Identification of ACSL4 as a biomarker and contributor of ferroptosis, Biochem. Biophys. Res. Commun 478 (2016) 1338–1343, 10.1016/j.bbrc.2016.08.124. [PubMed: 27565726]

[46]. Muhoberac BB, Vidal R, Iron, ferritin, hereditary ferritinopathy, and neurodegeneration, Front. Neurosci 13 (2019) 1195, 10.3389/fnins.2019.01195. [PubMed: 31920471]

[47]. Liu C, Chen K, Wang H, Zhang Y, Duan X, Xue Y, He H, Huang Y, Chen Z, Ren H, Wang H, Zeng C, Gastrin attenuates renal Ischemia/Reperfusion injury by a PI3K/Akt/Bad-mediated anti-apoptosis signaling, Front. Pharmacol 11 (2020), 540479, 10.3389/fphar.2020.540479. [PubMed: 33343341]

[48]. Doyle JF, Forni LG, Acute kidney injury: short-term and long-term effects, Crit. Care 20 (2016) 188, 10.1186/s13054-016-1353-y. [PubMed: 27373891]

[49]. Alomari M, TRIM21 - a potential novel therapeutic target in cancer, Pharmacol. Res 165 (2021), 105443, 10.1016/j.phrs.2021.105443. [PubMed: 33508433]

[50]. Lee KH, Tseng WC, Yang CY, Tarng DC, The anti-inflammatory, anti-oxidative, and anti-apoptotic benefits of stem cells in acute ischemic kidney injury, Int. J. Mol. Sci 20 (2019), 10.3390/ijms20143529.

[51]. Yoshimi R, Chang TH, Wang H, Atsumi T, Morse III HC, Ozato K, Gene disruption study reveals a nonredundant role for TRIM21/Ro52 in NF-kappaB-dependent cytokine expression

in fibroblasts, J. Immunol 182 (2009) 7527–7538, 10.4049/jimmunol.0804121. [PubMed: 19494276]

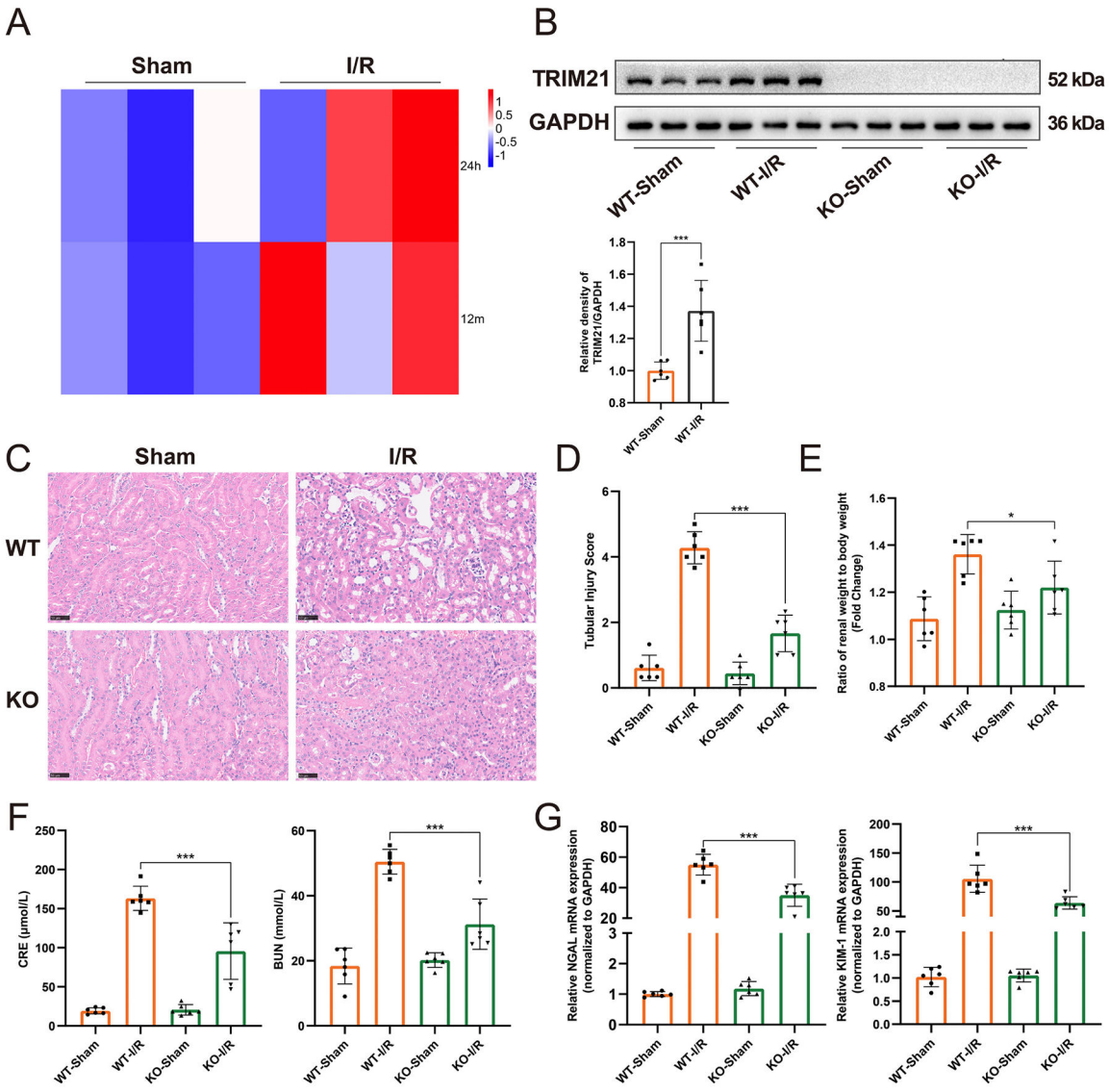

Fig. 1.

Loss of TRIM21 alleviates I/R-induced renal injury *in vivo*. (A) Heatmap of *Trim21* expression profiles were identified in mouse models at 24 h and 12 m after I/R-injury (n = 3). (B) In the I/R group, mice underwent 30 min of renal ischemia and 24 h of reperfusion (n = 6). Expression of TRIM21 in I/R-AKI mice were detected by western blot. (C–D) H&E staining of kidney tissues after I/R. Scale bars, 50 μm. The renal tubular injury score (scale: 0–5) was used to grade damage. (E) The ratio of renal weight to body weight was calculated. (F) Serum levels of CRE and BUN. (G) Quantification of kidney NGAL and KIM-1 mRNA levels by RT-qPCR. All data are expressed as the mean ± SD, *$p < 0.05$, ***$p < 0.001$.

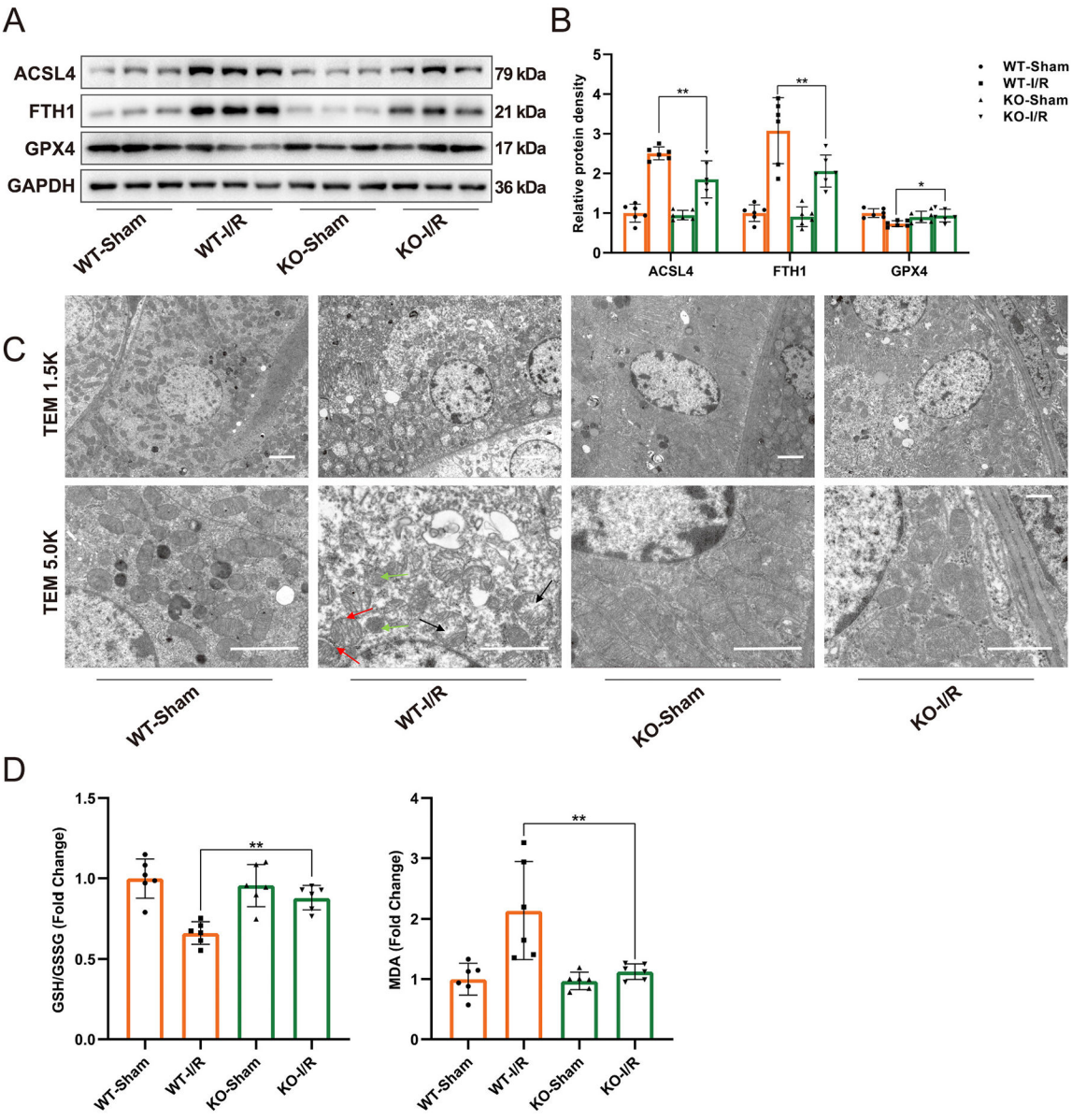

Fig. 2.

Loss of TRIM21 ameliorates ferroptosis in AKI caused by I/R. In the I/R group, mice underwent 30 min of renal ischemia and 24 h of reperfusion (n = 6). (A) Expression of ACSL4, FTH1, and GPX4 in I/R-AKI mice were detected by western blot. (B) Protein quantification. (C) Representative transmission electron micrographs show the ultrastructure of kidney tissues. Green, mitochondria shrink; red, the mitochondrial membrane thickens; black, the cristae decrease or disappear. Scale bars, 1 μm. (D) Levels of GSH/GSSG and MDA. All data are expressed as the mean ± SD, *$p < 0.05$, **$p < 0.01$, ***$p < 0.001$.

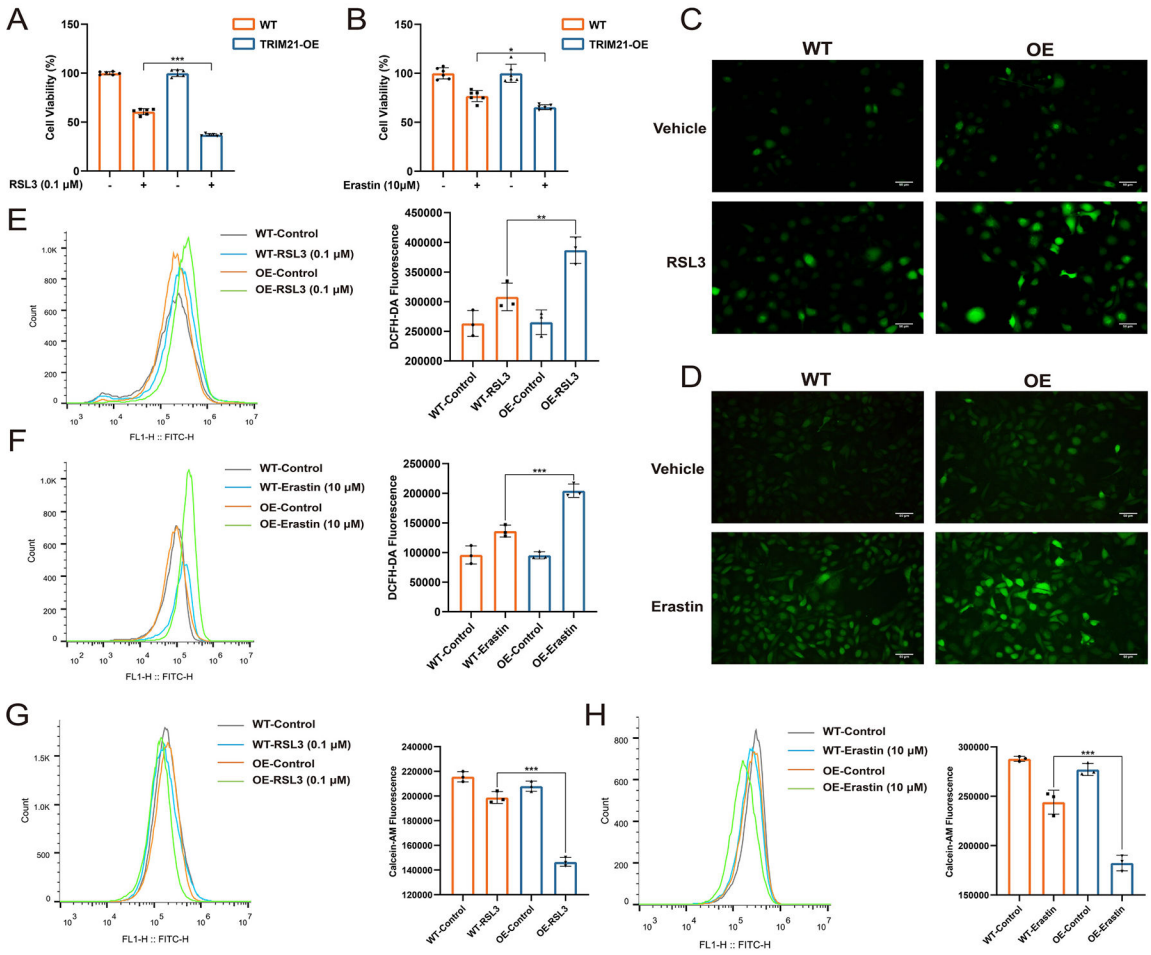

Fig. 3.

TRIM21 mediates the sensitivity to ferroptosis in HK-2 cells. TRIM21^{WT} and TRIM21^{OE} HK-2 cells were treated with RSL3 (0.1 μM) or Erastin (10 μM) for 24 h. (A–B) The cell viability was assessed by CCK-8 assay (n = 6). (C–D) Cellular ROS production was evaluated using a DCFH-DA fluorescent probe. Representative images are shown. Scale bars, 50 μm. (E–F) Cellular ROS was measured with a DCFH-DA fluorescent probe using flow cytometry (n = 3). (G–H) Intracellular iron levels were measured with calcein-AM, using flow cytometry (n = 3). All data are expressed as the mean ± SD, *$p < 0.05$, **$p < 0.01$, ***$p < 0.001$.

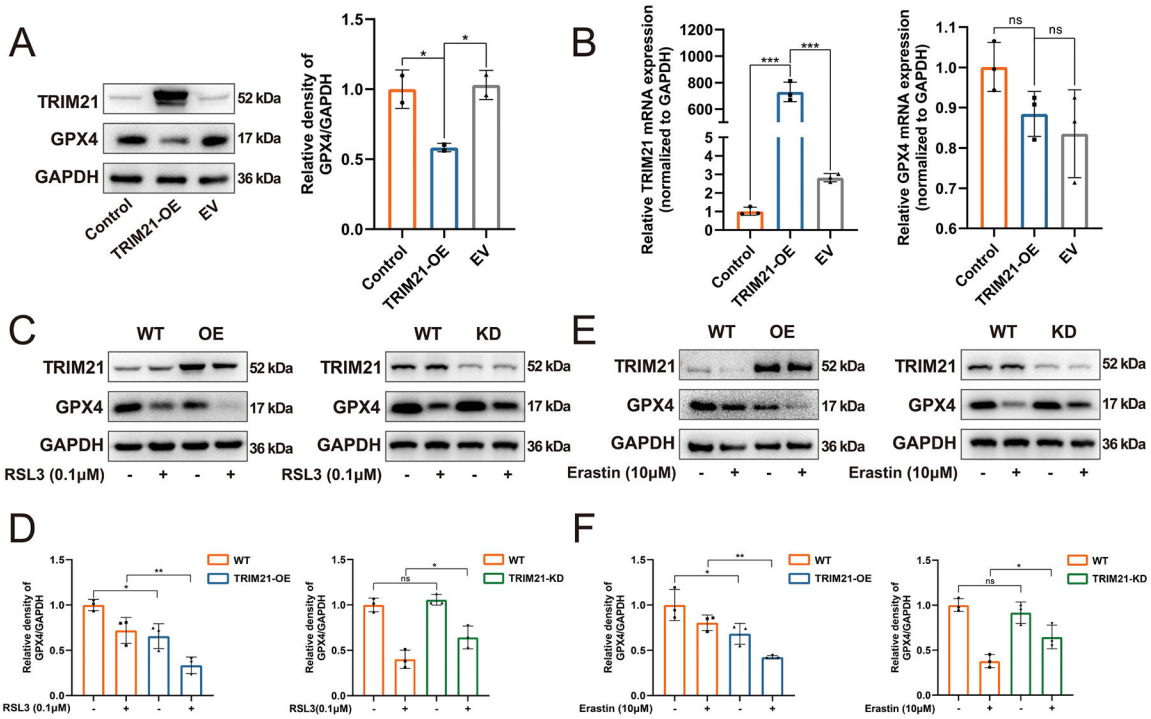

Fig. 4.

TRIM21 negatively regulates GPX4 at the protein level. (A) HK-2 cells were transfected with Myc-TRIM21 or EV plasmids (2 μg) for 24 h, and expression of TRIM21 and GPX4 were detected by western blot (n = 3). (B) Quantification of TRIM21 and GPX4 mRNA levels by RT-qPCR (n = 3). (C) $TRIM21^{WT}$, $TRIM21^{OE}$, and $TRIM21^{KD}$ HK-2 cells were treated with RSL3 (0.1 μM) for 24 h. (D) Protein quantification (n = 3). (E) $TRIM21^{WT}$, $TRIM21^{OE}$, and $TRIM21^{KD}$ HK-2 cells were treated with Erastin (10 μM) for 24 h. (F) Protein quantification (n = 3). All data are expressed as the mean ± SD, $*p < 0.05$, $**p < 0.01$, $***p < 0.001$.

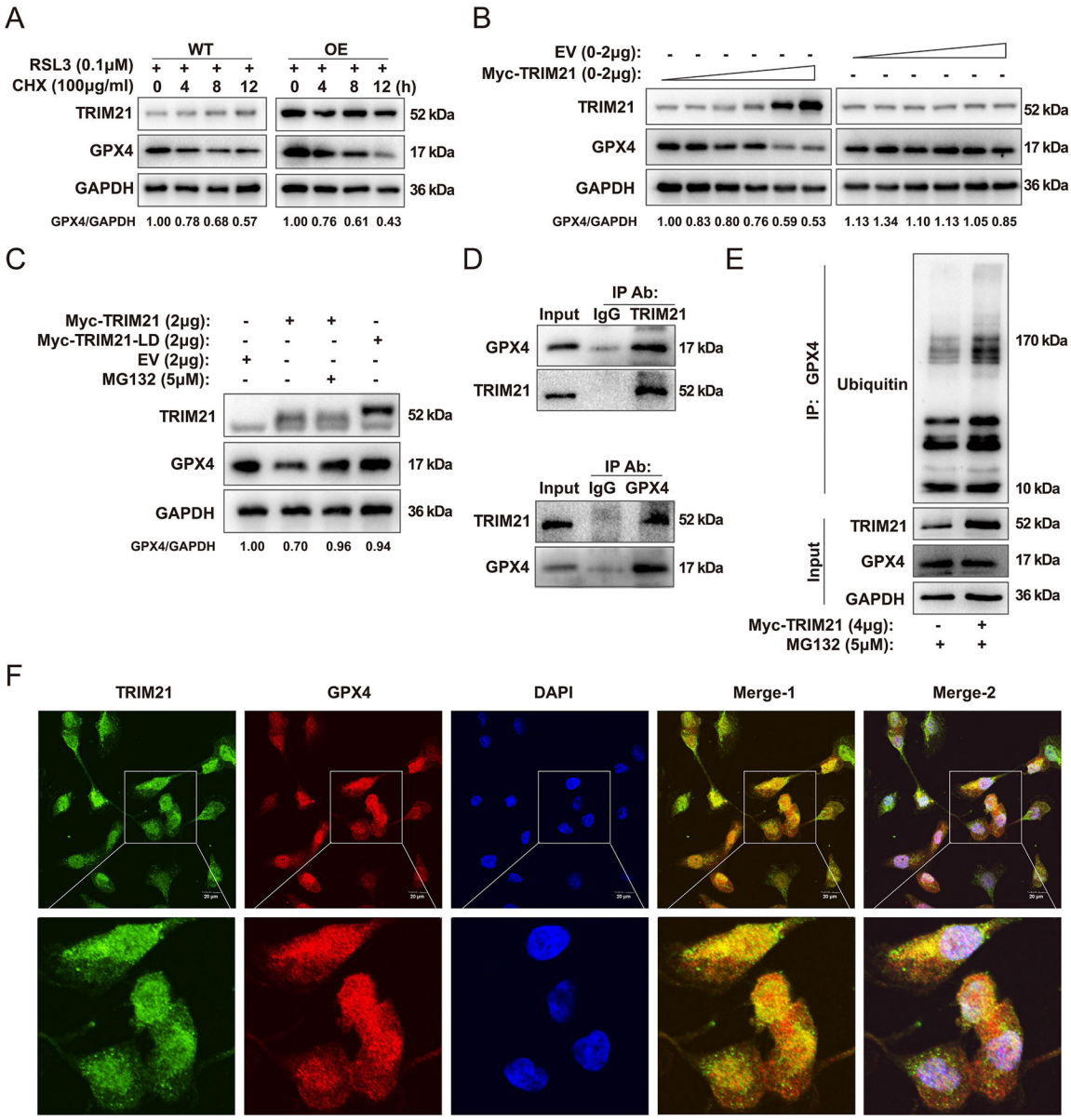

Fig. 5.

GPX4 is degraded by TRIM21-mediated ubiquitination. (A) TRIM21^{WT} and TRIM21^{OE} HK-2 cells were treated with RSL3, and then treated with CHX for 0 h, 4 h, 8 h, and 12 h, respectively. (B) Increasing doses of Myc-TRIM21 or EV plasmids were transfected into HK-2 cells for 24 h. (C) Myc-TRIM21 plasmids, Myc-TRIM21-LD plasmids, or EV plasmids were transfected into HK-2 cells for 24 h, then cells which transfected with Myc-TRIM21 plasmids treated with MG132 for 8 h. (D) The co-IP assay showed the interaction between TRIM21 and GPX4 in HK-2 cells. (E) Myc-TRIM21 plasmids were transfected into HK-2 cells in a 60 mm dish. After 24 h, MG132 was exposed to cells for 8 h. The cell lysates were subjected to analysis by IP, followed by IB detection. (F) Immunofluorescence staining revealed the co-localization of TRIM21 and GPX4 proteins in HK-2 cells. TRIM21 (green) and GPX4 (red) and nuclear (blue). Scale bars, 20 μm.

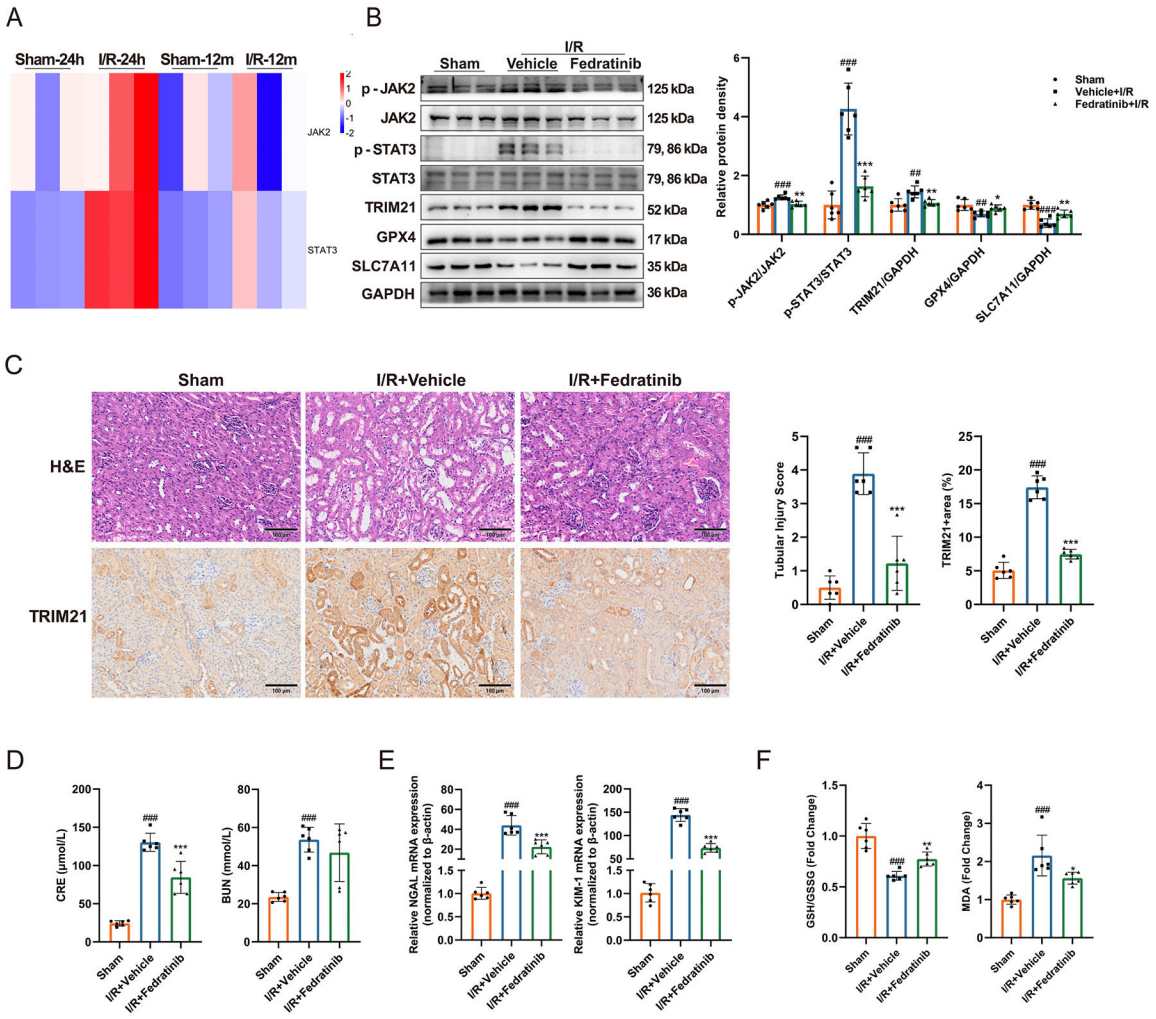

Fig. 6.

JAK2 inhibitor Fedratinib alleviates ferroptosis by down-regulating TRIM21 *in vivo*. (A) Heatmap of JAK2 and STAT3 expression profiles were identified in mouse models at 24 h and 12 m after I/R-injury (n = 3). (B) In the I/R group, mice underwent 30 min of renal ischemia and 24 h of reperfusion (n = 6). Expression of p-JAK2, JAK2, p-STAT3, STAT3, TRIM21, GPX4 and SLC7A11 in I/R-AKI mice among different groups detected by western blot. (C) H&E and immunohistochemistry staining of kidney tissues after I/R. Scale bars, 100 μm. The renal tubular injury score (scale: 0–5) was used to grade damage. (D) Serum levels of CRE and BUN. (E) Quantification of kidney NGAL and KIM-1 mRNA levels by RT-qPCR. (F) Levels of GSH/GSSG and MDA. $^{\#\#}p < 0.01$, $^{\#\#\#}p < 0.001$ compared with sham groups; $^{*}p < 0.05$, $^{**}p < 0.01$, $^{***}p < 0.001$ compared with vehicle groups.

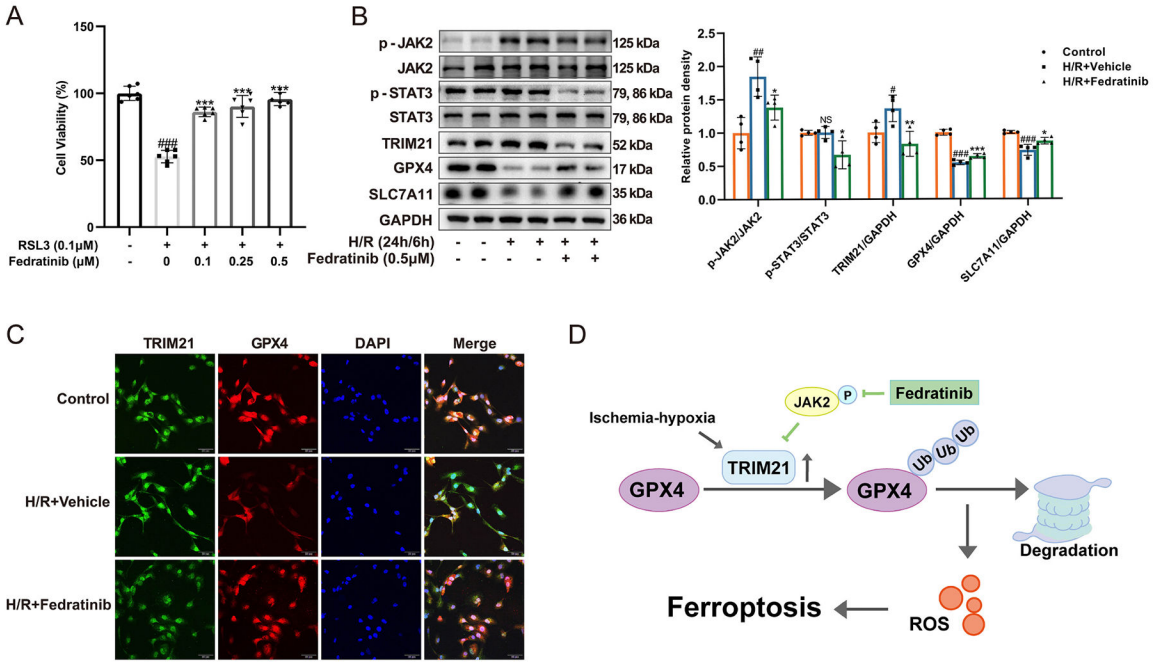

Fig. 7.

JAK2 inhibitor Fedratinib alleviates ferroptosis by down-regulating TRIM21 *in vitro*. (A) Co-treatment of HK-2 cells with RSL3 and Fedratinib for 24 h, and the cell viability was assessed by CCK-8 assay (n = 6). (B) HK-2 cells were treated with Fedratinib before H/R injury. Expression of p-JAK2, JAK2, p-STAT3, STAT3, TRIM21, GPX4, and SLC7A11 detected by western blot (n = 4). (C) Expression of TRIM21 and GPX4 detected by immunofluorescence. TRIM21 (green) and GPX4 (red) and nuclear (blue). Scale bars, 50 μm. All data are expressed as the mean ± SD. (D) Schematic diagram of the regulation of TRIM21 in I/R-AKI. TRIM21 was expressed at elevated levels in the I/R-AKI model *in vivo* and H/R model *in vitro*, while promoting ubiquitinated degradation of GPX4 and thus exacerbating ferroptosis by exerting E3 ubiquitin ligase activity. The JAK2 inhibitor Fedratinib could alleviate ferroptosis and AKI by inhibiting TRIM21, $^{\#}p < 0.05$, $^{\#\#}p < 0.01$, $^{\#\#\#}p < 0.001$ compared with control groups; $^{*}p < 0.05$, $^{**}p < 0.01$, $^{***}p < 0.001$ compared with RSL3 or vehicle groups.

Table 1

Information of primers.

Gene name	Forward	Reverse
human-TRIM21	5′ -TCAGCAGCACGCTTGACAAT-3′	5′-GGCCACACTCGATGCTCAC-3′
human-GPX4	5′-CCGCTGTGGAAGTGGATGAAGATC-3′	5′-CTTGTCGATGAGGAACTGTGGAGAG-3′
human-GAPDH	5′-GGGGAGCCAAAAGGGTCATCATCT-3′	5′-GAGGGGCCATCCACAGTCTTCT-3′
mouse-*Trim21*	5′-TGGTGGAGCCTATGAGTATCG-3′	5′-GGCACTCGGGACATGAACTG-3′
mouse-GPX4	5′-AGGCAGGAGCCAGGAAG-3′	5′-CCTTGGGCTGGACTTTC-3′
mouse-KIM-1	5′-ATCCCATACTCCTACAGACT-3′	5′-CCAACATAGAAGCCCTTA-3′
mouse-NGAL	5′-AAGGCAGCTTTACGATGT-3′	5′-TGGTTGTAGTCCGTGGTG-3′
mouse-β-actin	5′-GTGACGTTGACATCCGTAAAGA-3′	5′-GCCGGACTCATCGTACTCC-3′

Table 2

Information of plasmids.

Plasmids name	Vector	Type
human-TRIM21	pCDH-CMV-MCS-EF1-copGFP	Overexpression plasmid (for lentivirus infection)
human-TRIM21	pCMV3-ORF-Myc	Overexpression plasmid
human-TRIM21-ligase dead	pLNCX2 FR ras	Overexpression plasmid
human-TRIM21	Plenticrispr v2	SgRNA plasmid